



<http://www.diva-portal.org>

## Postprint

This is the accepted version of a paper published in *Applied Physics Letters*. This paper has been peer-reviewed but does not include the final publisher proof-corrections or journal pagination.

Citation for the original published paper (version of record):

Johansson, F., Ahlberg, P., Jansson, U., Zhang, S-L., Lindblad, A. et al. (2017)

Minimizing sputter-induced damage during deposition of WS<sub>2</sub> onto graphene.

*Applied Physics Letters*, 110(9): 091601

<https://doi.org/10.1063/1.4977709>

Access to the published version may require subscription.

N.B. When citing this work, cite the original published paper.

Permanent link to this version:

<http://urn.kb.se/resolve?urn=urn:nbn:se:uu:diva-316602>

Minimizing sputter-induced damage during deposition of WS<sub>2</sub> onto grapheneFredrik O. L. Johansson,<sup>1, a)</sup> Patrik Ahlberg,<sup>2</sup> Ulf Jansson,<sup>3</sup> Shi-Li Zhang,<sup>2</sup> Andreas Lindblad,<sup>1</sup> and Tomas Nyberg<sup>2, b)</sup><sup>1</sup>Department of Physics and Astronomy, Molecular and Condensed Matter Physics, Uppsala University, Box 516, SE-75120 Uppsala, Sweden<sup>2</sup>Division of Solid-State Electronics, The Ångström Laboratory, Uppsala University, Box 534, SE-75121 Uppsala, Sweden<sup>3</sup>Department of Chemistry, Inorganic Chemistry, Uppsala University, Box 538, SE-75121 Uppsala, Sweden

(Dated: February 3, 2017)

We demonstrate sputter-deposition of WS<sub>2</sub> onto a single-layer graphene film leaving the latter disorder-free. The sputtering process normally causes defects to the graphene lattice and adversely affects its properties. Sputtering of WS<sub>2</sub> yields significant amounts of energetic particles, specifically negative S ions and reflected neutral Ar, and it is therefore used as a model system in this work. The disorder-free sputtering is achieved by increasing the sputtering pressure of Ar thereby shifting the kinetic energy distribution towards lower energies for the impinging particle flux at the substrate. Raman spectroscopy is used to assess the amount of damage to the graphene film. Monte Carlo simulations of the sputtering process show that W is completely thermalized already at relatively low sputtering pressure, whereas Ar and S need comparably higher pressure to thermalize so as to keep the graphene film intact. Apart from becoming completely amorphous at 2.3 mTorr, the graphene film remains essentially disorder-free when the pressure is increased to 60 mTorr. The approach used here is generally applicable and readily extendable to sputter-deposition of other material combinations onto sensitive substrates. Moreover, it can be used without changing the geometry of an existing sputtering setup.

Graphene, with its extraordinary electronic, optical, thermal, and mechanical properties,<sup>1</sup> has attracted enormous interest within the scientific and engineering community both from fundamental and applied perspectives. In order to make functional devices, it is commonly required to deposit materials onto graphene without damaging it;<sup>2</sup> damage can also be used as a means to tailor chemical doping/functionalization.<sup>3</sup> This is not a trivial problem since the atomically thin layer of C, though one of the strongest materials known, is easily damaged by moderately energetic particles.<sup>4</sup>

There are several kinds of defects that can be induced in graphene by energetic particles. As described in detail by Ahlberg *et al.*<sup>4</sup>, there is no well-defined lower limit below which ions do not damage graphene. There is, however, a threshold energy at which graphene go from barely unaffected to amorphous. This threshold is element specific and it is experimentally determined to be 26 eV for Ar.<sup>4</sup> Moreover, the level of damage is dependent on the total number of energetic particles, *i.e.* the dose, before the deposit reaches a critical thickness beyond which the impinging atoms/ions do not interact with the underlying graphene film.

A scalable and commonly used industrial deposition technique is Physical Vapor Deposition (PVD) by DC magnetron sputtering. However, this process involves several types of energetic particles that may damage graphene sheets.<sup>4-6</sup> They consist of atoms sputtered of

the target, Ar reflected from the target, and negative ions created at the target.

To lower the kinetic energy of these particles, the Ar pressure can be increased. The energetic particles from the target will interact with Ar and their kinetic energies will decrease as a result of frequent collisions. To avoid exposure to graphene of these particles, several schemes have been proposed; having the substrate facing away from the target allows only thermalized particles to reach the surface<sup>7,8</sup>, and analogously the substrate can be placed perpendicular to the target<sup>5</sup>. It has also been shown that limiting the flux of Au atoms by shielding and increasing the sputtering pressure yields conditions compatible with device production.<sup>9</sup> In addition to the deterioration of graphene by energetic particles, chemical reactions may also damage the material.<sup>7,10</sup>

In this paper, we investigate experimentally how sputter damage in graphene can be minimized during sputter-deposition of WS<sub>2</sub> from a WS<sub>2</sub> target in pure Ar. The experimental results are further compared with simulated kinetic energy and kinetic energy distributions of ions and neutral atoms arriving at the film obtained using a Monte-Carlo based approach.<sup>11,12</sup> The amount of structural damage in graphene is determined by Raman spectroscopy, which is sensitive to defects in graphene.<sup>13</sup> It is demonstrated that increasing the sputtering pressure shifts the whole particle kinetic energy distribution towards lower energies, with an increasingly large part being below the threshold of ejecting C atoms from the graphene lattice.

The graphene films were grown by means of Chemical Vapor Deposition (CVD) onto Cu foil, using a gas mixture of Ar:H<sub>2</sub>:CH<sub>4</sub>. The deposition was carried out

<sup>a)</sup>fredrik.johansson@physics.uu.se<sup>b)</sup>tomas.nyberg@angstrom.uu.se

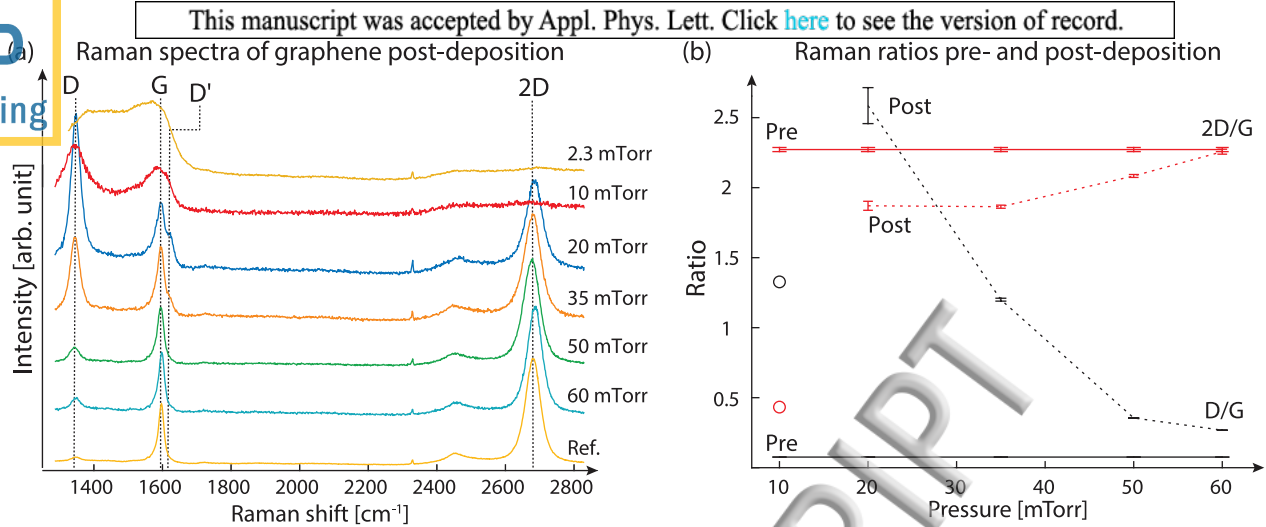


Figure 1. (a) Representative Raman spectra at various pressures together with a reference spectrum of the pre-deposition material. (b) The 2D/G and D/G ratios for the sputter-deposited films, as well as for the as-transferred graphene prior to deposition. The circles indicate ratios for 10 mTorr disconnected from the other points in the series since the material is completely amorphous, with a 2D/G ratio of  $\sim 0.5$  and a D/G ratio of  $\sim 1.3$ .

72 in a diffusion furnace at 1000 °C and 1.4 Torr. The films  
73 were transferred, using a previously described residue free  
74 transfer method onto a thermally oxidised Si wafer hav-  
75 ing a 300 nm thick SiO<sub>2</sub> layer.<sup>14</sup> This approach is chosen  
76 because it is the viable manufacturing technique for in-  
77 dustrial scale production of graphene.<sup>15</sup>

78 All WS<sub>2</sub> coatings were sputter-deposited by magnetron  
79 sputtering in a high vacuum CS 600 von Ardenne sys-  
80 tem. The base pressure for all depositions was in the 10<sup>-7</sup>  
81 mTorr range. A 100 mm WS<sub>2</sub> sputter target (K. Lesker  
82 Inc.) with purity of 99.9%, was used with a pulsed DC  
83 power at 200 W. Ar was used as sputtering gas at a flow  
84 rate of 20 sccm. The processing pressure was varied from  
85 2.3 mTorr to 60 mTorr with the deposition time adjusted  
86 so as to achieve a 5 nm thick WS<sub>2</sub> film on each sample.  
87 The deposition rate varied between 9 nm/min, at the  
88 lowest processing pressure, and 4 nm/min, at the highest  
89 pressure. The magnetron was located on the top lid of  
90 the deposition chamber with a 30° angle towards the sub-  
91 strate table at the center of the chamber bottom. The  
92 target to substrate distance was 16 cm. The graphene  
93 coated SiO<sub>2</sub>/Si samples were located in front of the tar-  
94 get at the conventional substrate position, *i.e.* on-axis in  
95 front of the target.

96 All WS<sub>2</sub> films were characterized by means of x-  
97 ray photoelectron spectroscopy (XPS) using a Physical  
98 Systems Quantum 2000 spectrometer with monochro-  
99 matic AlK $\alpha$  radiation. XPS data indicate an under-  
100 stoichiometric WS<sub>2-x</sub> at low processing pressure, whilst  
101 approaching stoichiometric WS<sub>2</sub> above 50 mTorr. Each  
102 sample was characterized before and after the WS<sub>2</sub> de-  
103 position using Raman spectroscopy (Renishaw "inVia"  
104 Raman spectrometer) with 532 nm laser excitation at  
105 20x magnification.

106 In Figure 1(a), the Raman spectra for graphene at dif-

107 ferent processing pressures are exhibited; at the bottom  
108 of the graph a spectrum of the as-grown graphene trans-  
109 ferred onto an oxidized Si substrate is included as refer-  
110 ence. For detailed interpretation of the Raman spectra  
111 and the labelling of the peaks, D, G, D' and 2D, see Fer-  
112 rari *et al.*<sup>16</sup>. The small peak at 2330 cm<sup>-1</sup> comes from  
113 the N<sub>2</sub> gas present in the ambient air.<sup>17</sup> The amount  
114 of induced damage in the graphene film is assessed by  
115 analyzing the Raman spectra in the following way: the  
116 ratio of the max intensity of the D peak to that of the  
117 G peak (D/G) is used as a measure of the amount of  
118 damage to graphene. This ratio is inversely correlated to  
119 the distance between two lattice defects, whereas the 2D  
120 to G ratio (2D/G) identifies the resemblance to mono-  
121 layer graphene.<sup>4,13,16,18</sup> At the lowest pressures, *i.e.* 2.3  
122 and 10 mTorr, the spectra are significantly different from  
123 the reference spectrum, indicative of amorphization.<sup>4</sup>  
124 At 20 mTorr, the spectrum shows clear D, D' and 2D  
125 peaks, indicative of heavily damaged, but not amorph-  
126 ized, graphene. With increasing pressure, the D and  
127 D' peaks become fainter while the G and 2D peaks keep  
128 their intensity and also become narrower, which is an  
129 indication of low-defect density graphene.<sup>4,16</sup>

130 Sputtering at pressure above 60 mTorr resulted in  
131 spontaneous and randomly occurring discharges around  
132 the substrate table. Therefore, 60 mTorr is our highest  
133 processing pressure in this study. This upper limit of  
134 the pressure is dependent on the chamber geometry and  
135 process parameters used and can vary for other systems  
136 than the presently studied.

137 For the 2D/G and D/G ratios summarized in Figure  
138 1(b), the maximum intensity of the peaks is used. More-  
139 over, the peaks are fitted with Voigt profiles and a linear  
140 background in MATLAB using the inbuilt least-squares  
141 fit procedure. Each data point represents an average of  
142 up to 100 spectra collected on the sample. Analyzing

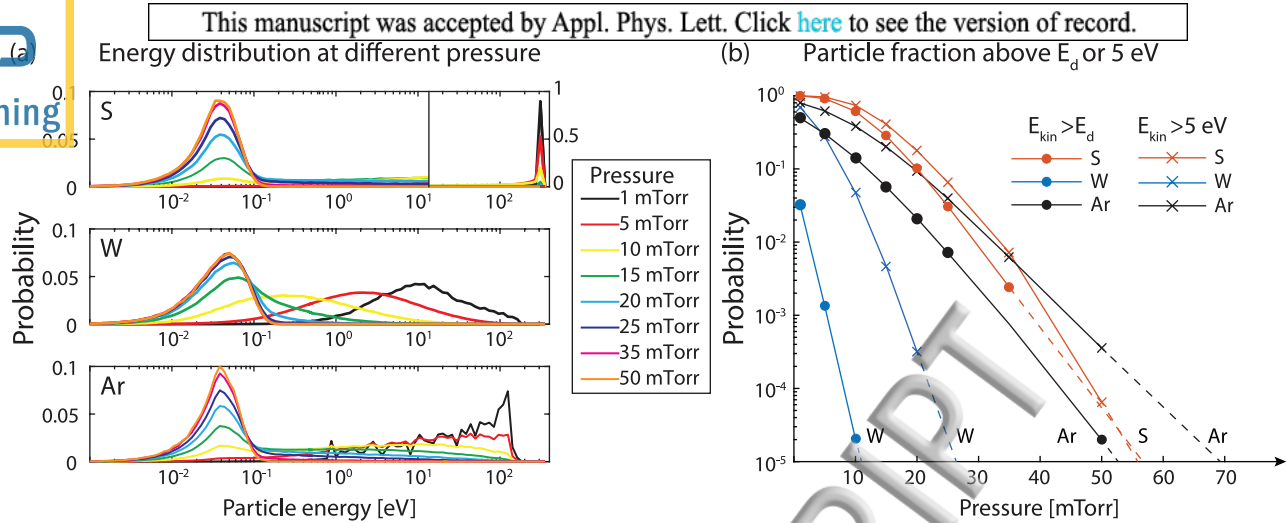


Figure 2. (a) Distribution of kinetic energy at different sputtering pressure for sputtered W neutral atoms, S negative ions, and reflected Ar involved in the deposition process. Note the logarithmic scale on the energy axis and the different scale on the probability axis for energies above 10 eV in the energy distribution for S (as indicated by the solid line at 10 eV). (b) Probability of atoms/ions having kinetic energies above  $E_d$  or 5 eV. The dashed lines are extrapolations serving as guides for the eye.

143 a series of spectra this way, we also get an estimate of 178 (5) the energy and direction of the atom is updated.  
 144 the variation of the sample as reflected in the error bars. 179 Steps (2)-(5) are repeated for each atom until it is  
 145 Most of the error bars are within the size of the markers, 180 adsorbed. Results from such simulations are illustrated  
 146 indicating that the homogeneity of the samples is good 181 in Figure 2(a) where the kinetic energy distribution  
 147 throughout the sample series. 182 is shown for the different atoms/ions arriving at the  
 183 substrate.

148 The horizontal line at the ratio 2.25 marked "Pre" 184 All simulations assume a simplified environment with  
 149 in Figure 1(b) indicates the 2D/G ratio from the as- 185 a flat target and flat substrate. In real life, the target will  
 150 transferred graphene, the line at 0.1 indicates the cor- 186 not have a flat radial distribution, a race-track like groove  
 151 responding D/G ratio. The D/G ratio marked "Post" 187 is formed after some usage. This will affect the initial  
 152 represents the results after sputter-deposition. It varies 188 distribution of energy and direction of the atoms emanat-  
 153 with processing pressure from a ratio of 2.5 at 20 mTorr 189 ing from the surface. However, at higher pressures this  
 154 to less than 0.5 above 50 mTorr. The 2D/G ratio marked 190 discrepancy will vanish due to large number collisions.  
 155 "Post" varies between 2 and 2.25 in the 20 to 60 mTorr 191 Furthermore, the mean free path of each atom/ion is cal-  
 156 range. The graphene films receiving the WS<sub>2</sub> deposition 192 culated assuming a complete thermalization. This ap-  
 157 at 2.3 and 10 mTorr were also analyzed, but as the 193 proach will somewhat underestimate the mean free path  
 158 films were completely destroyed only the 10 mTorr data 194 for high energy particles.<sup>11</sup> The interaction between the  
 159 points are shown (as disconnected circles) in Figure 1(b). 195 particles is described with a hard sphere potential, which  
 160 Above 50 mTorr, both the 2D/G and D/G ratios reach 196 may also be considered a simplification compared to, *e.g.*,  
 161 a regime where the graphene is only slightly damaged by 197 the Lennard-Jones potential. But at the kinetic energies  
 162 the sputtering process. 198 considered here, this simplification does not affect the  
 199 scattering properties in the collisions significantly. De-  
 200 spite approximations and idealizations outlined above,  
 201 the same code has previously been used to successfully  
 202 describe compositional variations at different substrate  
 203 positions and pressures in the case of WS<sub>2-x</sub>.<sup>12</sup>

163 The particle energy distribution was obtained 198  
 164 by means of Monte-Carlo simulations, detailed 199  
 165 elsewhere.<sup>11,12,19</sup> In brief, (1) the initial energy and 200  
 166 direction of the sputtered W atoms and the reflected 201  
 167 Ar are calculated using SRIM<sup>20</sup>. Negative ions, in 202  
 168 this instance S, are given the target potential to define 203  
 169 their initial energy with a direction along the target 204  
 170 surface's normal towards the substrate; (2) each atom 205  
 171 then propagates a distance randomly generated using its 206  
 172 mean free path; (3) if the vector between the old and new 207  
 173 positions intersect a chamber wall (or substrate), the 208  
 174 particle regarded adsorbed and the impact position is 209  
 175 saved together with the energy; (4) if no wall/substrate 210  
 176 adsorption occurs, a hard-sphere collision occurs with a 211  
 177 sputter gas atom (using theoretical atomic radii<sup>21</sup>); and 212

213 W, S and Ar. For the heavier element, this peak appears  
214 at lower pressure since the collision cross-section is larger  
215 giving rise to a comparatively larger number of  
216 collisions on the way to the substrate.

217 A high energy tail can be seen for both S and Ar, al-  
218 though much more pronounced for Ar. These particles  
219 are the ones with sufficient kinetic energy to damage the  
220 graphene film. To ascertain if S or Ar is the main culprit,  
221 one would need to determine the flux of the particles by  
222 multiplying the number of particles per unit time of each  
223 kind with their energy distribution. It is not straightfor-  
224 ward to estimate an exact number of the different partic-  
225 les, but calculations using SRIM estimate that sputtered  
226 S and W atoms and reflected Ar are present at the tar-  
227 get with an approximate proportion of 4/2/1. With the  
228 experimental conditions used, only a very small fraction  
229 of the the sputtered S atoms are negatively ionized at  
230 the target surface. These ions, are (much) fewer com-  
231 pared to the number of reflected Ar atoms. This points  
232 toward the reflected Ar as the main cause of the damage  
233 to graphene for the considered system at higher pressure.

234 In Figure 2(b), the fraction of particles having a kinetic  
235 energy above the displacement energy ( $E_d$  in Equation 1)  
236 or above 5 eV, that hit the substrate are plotted. The two  
237 thresholds are chosen to identify energetic atoms/ions  
238 that can create different types of defects.  $E_d$  is the min-  
239 imum kinetic energy of a projectile required to remove a  
240 C atom from a free standing graphene sheet. To calcu-  
241 late  $E_d$  for a given atom, the expression for the maximum  
242 energy transferred in an elastic collision is used:

$$E_d = \frac{T_d(m_c + M)^2}{4m_cM} \quad (1)$$

243 Here,  $T_d$  is the lowest energy required to displace a C  
244 atom in graphene and it is calculated to be 22.2 eV<sup>22,23</sup>,  
245  $m_c$  and  $M$  are the mass of a C atom and the incoming  
246 atom, respectively.  $E_d$  for Ar, W, and S are calculated  
247 to be 31.2, 96.4, and 28.0 eV, respectively. It has also  
248 been demonstrated that graphene may become damaged  
249 from particles having significantly lower energies than  
250  $E_d$ .<sup>4</sup> Particles with a few eV of kinetic energy may cre-  
251 ate the Stone-Wales type of defects that can deteriorate  
252 graphene at high doses. Therefore, we have chosen 5 eV  
253 as the lower energy threshold for this defect formation  
254 mechanism.

255 The complete thermalization of W is achieved at rel-  
256 atively low sputtering gas pressure, whereas the lighter  
257 atoms/ions stay energetic at higher pressure. It can also  
258 be seen that the amount of Ar with energies above 5 eV  
259 has a lower decline rate than the amount of S with ener-  
260 gies above 5 eV.

261 Comparing Figure 1(b) and 2(b), the same trend is ob-  
262 served for both the D/G ratio and the probability. When  
263 the probability of particles with an energy above  $E_d$  is  
264 high, the high D/G ratio indicates damaged graphene.  
265 When the sputtering pressure is increased and the prob-  
266 ability of particles with energies above  $E_d$  decreases, the  
267 D/G ratio also decreases. At 50 mTorr, all W atoms

268 are thermalized, and thus are not contributing to dam-  
269 aging the graphene. However, both S and Ar still have  
270 a significant fraction of their kinetic energy distributions  
271 populated at energies that can damage the graphene film.  
272 At higher pressure there will be some, although at a low  
273 probability, particles with energy of several eV. This re-  
274 sult also points toward neutralized reflected Ar atoms as  
275 being the particles that are most likely to cause damage  
276 to graphene above 50 mTorr.

277 The deposited WS<sub>2</sub> films are of (nominal) equal thick-  
278 ness for all pressures, in order to attain doses of W and S  
279 unaffected by the processing pressure. The same should  
280 be true also for reflected Ar, since it has a mass and size  
281 similar to those of S. However, although the deposition  
282 time is more than doubled between the lowest and high-  
283 est pressure points, the graphene film is not damaged for  
284 60 mTorr – since the amount of high energy particles at  
285 the substrate is insignificant at the higher pressure.

286 The sputtering process may represent a rather difficult  
287 process to predict in great detail. As shown here, sev-  
288 eral kinds of particles can affect graphene during sputter-  
289 deposition. The energy distribution and amounts of the  
290 different species depend on the materials system. We  
291 choose to study sputter-deposition of WS<sub>2</sub> because sig-  
292 nificant amounts of negative ions and reflected Ar are  
293 generated at rather high energies. Other materials can  
294 give dramatically different flux and energy distribution  
295 of energetic particles. In general, our simulations show  
296 that an increase in the sputtering pressure will effectively  
297 thermalize W and S, as can be seen in Figure 2, whereas  
298 a non-negligible amount of reflected Ar retains energies  
299 above 5 eV. Our experimental results, verified by exten-  
300 sive simulations, show a clear trend of decreasing damage  
301 at higher processing pressure.

302 In conclusion, we have shown that sputtering com-  
303 pound films onto graphene with controlled damage is  
304 possible by increasing the sputtering pressure and not re-  
305 quiring special substrate geometry or holders. Although  
306 WS<sub>2</sub> has been used in this work, the findings are ap-  
307 plicable also to other transition metal dichalcogenides,  
308 *e.g.* MoS<sub>2</sub>, MoSe<sub>2</sub>, *etc.* Furthermore, we demonstrate  
309 that simulation can predict the suitable sputtering pres-  
310 sure regime and that the sputtering gas is a key factor in  
311 keeping the sputter damage to a minimum.

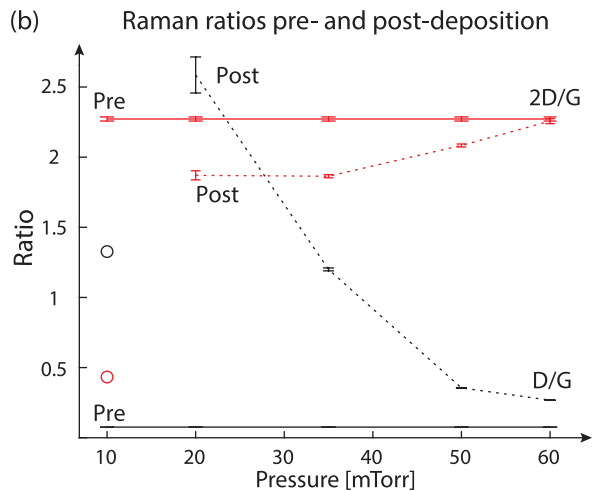
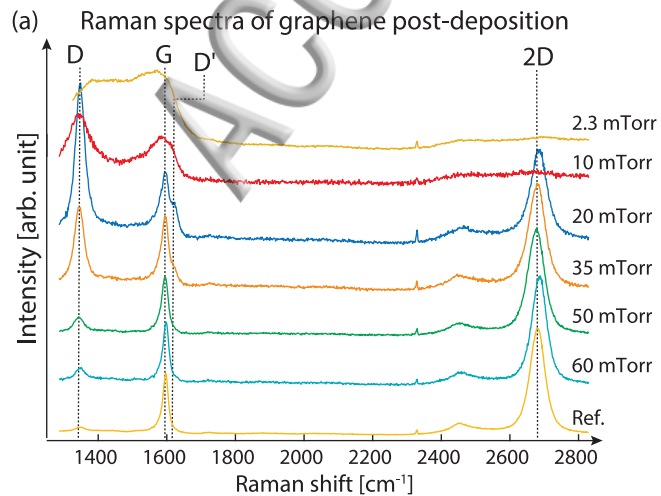
312 The simulation results shown here are tailored for the  
313 sputtering and materials system used. This allows us to  
314 draw quantitative conclusions regarding the critical pres-  
315 sure at which S, W, or Ar can be thermalized. Since bom-  
316 bardment by energetic particles is material dependent, it  
317 is concluded that simulation is of importance in order to  
318 gain insight on what processing pressure is required for  
319 disorder-free sputtering onto graphene.

320 This work was financially supported in part by the  
321 Knut and Alice Wallenberg Foundation (No. 2011.0082),  
322 the Swedish Research Council (Nos. 2014-5591 and  
323 2014-6463), Marie Skłodowska Curie Actions, Cofund,  
324 Project INCA 600398 and Stiftelsen för Olle Engkvist  
325 Byggmästare (2016/39).

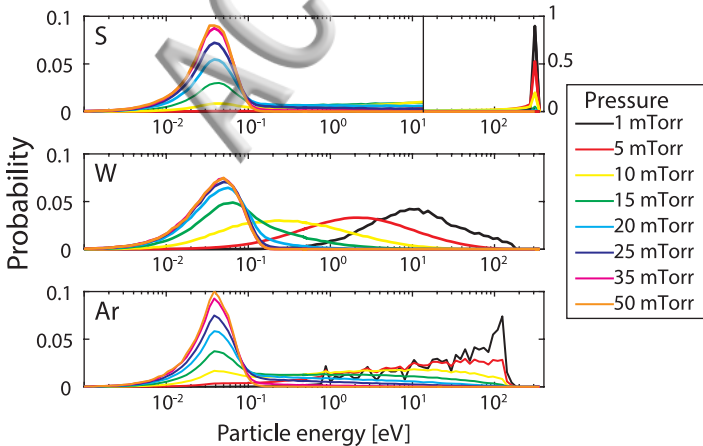
## REFERENCES

- 327 A. C. Ferrari, F. Bonaccorso, V. Fal'ko, K. S. Novoselov,  
328 S. Roche, P. Boggild, S. Borini, F. H. L. Koppens, V. Palermo,  
329 N. Pugno, J. A. Garrido, R. Sordan, A. Bianco, L. Ballerini,  
330 M. Prato, E. Lidorikis, J. Kivioja, C. Marinelli, T. Ryhanen,  
331 A. Morpurgo, J. N. Coleman, V. Nicolosi, L. Colombo,  
332 A. Fert, M. Garcia-Hernandez, A. Bachtold, G. F. Schneider,  
333 F. Guinea, C. Dekker, M. Barbone, Z. Sun, C. Galiotis, A. N.  
334 Grigorenko, G. Konstantatos, A. Kis, M. Katsnelson, L. Vander-  
335 sypen, A. Loiseau, V. Morandi, D. Neumaier, E. Treossi, V. Pelle-  
336 grini, M. Polini, A. Tredicucci, G. M. Williams, B. Hee Hong, J.-  
337 H. Ahn, J. Min Kim, H. Zirath, B. J. van Wees, H. van der Zant,  
338 L. Occhipinti, A. Di Matteo, I. A. Kinloch, T. Seyller, E. Ques-  
339 nel, X. Feng, K. Teo, N. Rupesinghe, P. Hakonen, S. R. T. Neil,  
340 Q. Tannock, T. Lofwander, and J. Kinaret, *Nanoscale* **7**, 4598  
341 (2015).
- 342 <sup>2</sup>T. Georgiou, R. Jalil, B. D. Belle, L. Britnell, R. V. Gor-  
343 bachev, S. V. Morozov, Y.-J. Kim, A. Gholinia, S. J. Haigh,  
344 O. Makarovsky, L. Eaves, L. A. Ponomarenko, A. K. Geim, K. S.  
345 Novoselov, and A. Mishchenko, *Nat. Nanotechnol.* **8**, 100 (2013).
- 346 <sup>3</sup>H. Li, L. Daukiya, S. Haldar, A. Lindblad, and B. Sanyal, *Sci.*  
347 *Rep.* **6**, 19719 (2016).
- 348 <sup>4</sup>P. Ahlberg, F. O. L. Johansson, Z.-B. Zhang, U. Jansson, S.-  
349 L. Zhang, A. Lindblad, and T. Nyberg, *APL Mater.* **4**, 046104  
350 (2016).
- 351 <sup>5</sup>C. T. Chen, E. A. Casu, M. Gajek, and S. Raoux, *Appl. Phys.*  
352 *Lett.* **103**, 2011 (2013).
- 353 <sup>6</sup>S. M. Rosnagel, *J. Vac. Sci. Technol. A* **7**, 1025 (1989).
- 354 <sup>7</sup>X. P. Qiu, Y. J. Shin, J. Niu, N. Kulothungasagaran, G. Kalon,  
355 C. Qiu, T. Yu, and H. Yang, *AIP Adv.* **2**, 032121 (2012),  
356 1208.1835.
- 357 <sup>8</sup>M. Jamali, Y. Lv, Z. Zhao, and J. P. Wang, *AIP Adv.* **4**, 107102  
358 (2014).
- 359 <sup>9</sup>B. Li, G. Pan, N. Y. Jamil, L. Al Taan, S. Awan, and N. Avent,  
360 *J. Vac. Sci. Technol. A* **33**, 030601 (2015).
- 361 <sup>10</sup>P. Ahlberg, T. Nyberg, S.-L. Zhang, Z.-B. Zhang, and U. Jans-  
362 son, *J. Vac. Sci. Technol. B* **34**, 040605 (2016).
- 363 <sup>11</sup>E. Särhammar, E. Strandberg, N. Martin, and T. Nyberg, *Int.*  
364 *J. Mater. Sci. Appl.* **3**, 29 (2014).
- 365 <sup>12</sup>E. Särhammar, E. Strandberg, J. Sundberg, H. Nyberg,  
366 T. Kubart, S. Jacobson, U. Jansson, and T. Nyberg, *Surf. Coat.*  
367 *Technol.* **252**, 186 (2014).
- 368 <sup>13</sup>M. Lucchese, F. Stavale, E. M. Ferreira, C. Vilani, M. Moutinho,  
369 R. B. Capaz, C. Achete, and A. Jorio, *Carbon* **48**, 1592 (2010).
- 370 <sup>14</sup>M. Hinnemo, P. Ahlberg, C. Hägglund, W. Ren, H.-M. Cheng,  
371 S.-L. Zhang, and Z.-B. Zhang, *Carbon* **98**, 567 (2016).
- 372 <sup>15</sup>R. Muñoz and C. Gómez-Aleixandre, *Chem. Vap. Depos.* **19**, 297  
373 (2013).
- 374 <sup>16</sup>A. C. Ferrari and D. M. Basko, *Nat Nano* **8**, 235 (2013).
- 375 <sup>17</sup>M. A. Pimenta, G. Dresselhaus, M. S. Dresselhaus, L. G. Can-  
376 cado, A. Jorio, and R. Saito, *Phys. Chem. Chem. Phys.* **9**, 1276  
377 (2007).
- 378 <sup>18</sup>L. G. Cançado, A. Jorio, E. H. M. Ferreira, F. Stavale, C. A.  
379 Achete, R. B. Capaz, M. V. O. Moutinho, A. Lombardo, T. S.  
380 Kulmala, and A. C. Ferrari, *Nano Letters* **11**, 3190 (2011).
- 381 <sup>19</sup>E. Särhammar, *Sputtering and Characterization of Complex*  
382 *Multi-element Coatings*, Ph.D. thesis, Uppsala University (2014).
- 383 <sup>20</sup>J. F. Ziegler and J. P. Biersack, "Treatise on Heavy-Ion Science:  
384 Volume 6: Astrophysics, Chemistry, and Condensed Matter,"  
385 (Springer US, Boston, MA, 1985) Chap. The Stopping and Range  
386 of Ions in Matter, pp. 93–129.
- 387 <sup>21</sup>E. Clementi, D. L. Raimondi, and W. P. Reinhardt, *J. Chem.*  
388 *Phys.* **47**, 1300 (1967).
- 389 <sup>22</sup>O. Lehtinen, J. Kotakoski, A. V. Krasheninnikov, A. Tolvanen,  
390 K. Nordlund, and J. Keinonen, *Phys. Rev. B* **81**, 153401 (2010).
- 391 <sup>23</sup>A. Merrill, C. D. Cress, J. E. Rossi, N. D. Cox, and B. J. Landi,  
392 *Phys. Rev. B* **92**, 075404 (2015).

ACCEPTED MANUSCRIPT



(a) Energy distribution at different pressure



(b) Particle fraction above  $E_d$  or 5 eV

